Article

Vegetation Dynamics Due to Urbanization in the Coastal Cities along the Maritime Silk Road

Min Yan [1], Shunxiang Fan [2], Li Zhang [1,*], Riffat Mahmood [1,3,4], Bowei Chen [1] and Yuqi Dong [1,3]

[1] Key Laboratory of Digital Earth Sciences, Aerospace Information Research Institute, Chinese Academy of Sciences, No. 9 Dengzhuang South Road, Beijing 100094, China; yanmin@aircas.ac.cn (M.Y.); riffat.mahmood.jnu@gmail.com (R.M.); chenbw@aircas.ac.cn (B.C.); dongyuqi21@mails.ucas.ac.cn (Y.D.)
[2] College of Resources and Environmental Sciences, China Agricultural University, Beijing 100193, China; fansx@cau.edu.cn
[3] College of Resources and Environment, University of Chinese Academy of Sciences, Beijing 100049, China
[4] Department of Geography and Environment, Faculty of Life and Earth Sciences, Jagannath University, Dhaka 1100, Bangladesh
[*] Correspondence: zhangli@aircas.ac.cn; Tel.: +86-010-8217-8193

Abstract: Substantial research indicates the effects of urbanization on vegetation cover; however, a view of this scenario from a regional scale is absent. Nowadays, coastal cities have become the new engine for the development of countries in coastal areas. To capture the effects of rapid urbanization on vegetation dynamics, 35 coastal cities along the Maritime Silk Road (MSR) were selected to study the related research using quantitative tools. We calculated spatiotemporal trends of vegetation dynamics along an urban development intensity (UDI) gradient using the MODIS-enhanced vegetation index (EVI) during the period of 2000–2015. We found a significant reduction ($p < 0.05$) in the EVI in the core area against that in the rural area (ΔEVI) of 14 cities and an insignificant change in vegetation in the peri-urban areas or urban outskirts. EVI decreased significantly along the UDI gradients in 12 coastal cities with a linear pattern and in seven coastal cities with a concave pattern; only Bangkok exhibited a convex pattern. The nonlinear pattern between the EVI and UDI reflected the fact that vegetation dynamics were affected by complicated factors, including climate change and human interventions, over a long period of time. In conclusion, our work provided a scientific reference for the sustainable development of coastal cities along the MSR; further work is necessary to explore the mechanic details of the positive and negative influences of urban factors and related policies on vegetation conditions.

Keywords: coastal cities; Maritime Silk Road; urbanization; urban development intensity (UDI)

1. Introduction

In recent decades, urban centers have developed within coastal zones and cities, becoming an important part of the economy in these coastal states or provinces [1]. Coastal cities constitute critical gates into the hinterland, where they serve as economic centers that provide amenities and services for human-related activities, including tourism, transportation and fishing. Due to their special sea-level locations, coastal cities are vulnerable to flooding from rises in sea level, extreme weather and tsunamis. Therefore, more attention should be devoted to the sustainable development of coastal cities.

The Maritime Silk Road (MSR) is a sea trading route that has been rejuvenated economically by China as a strategy to boost economic and cultural connectivity throughout Southeast Asia, Oceania, the Indian Ocean and East Africa [2,3]. Being a sea channel, ports play important roles in economic development along the MSR. The shipping industry and port throughput have grown rapidly from 1990 to 2015 [4]; meanwhile, shipping networks for local ports have developed across space, and spatial linkages have enhanced the dependence of different sizes of ports. Coastal cities incorporate the functions of ports and

urban areas; therefore, the development of ports leads to the development of coastal cities. The rising scale and transportation of ports has marked the rapid expansion and economic development of coastal cities in recent decades [5]. This rapid urbanization often results in abrupt land-use changes that lead to the degradation of the natural environment, including reductions in vegetation [6], increased coastal erosion [7,8] and reduced ecosystem diversity [9].

Vegetation enacts important roles in urban systems, such as mitigating global warming [10], preventing water and soil loss [11] and alleviating city heat islands [12,13]. Coastal vegetation, including mangroves, salt marshes, macroalgae, seagrasses, coastal strands and dunes, also buffer shores and retain sediments from tides, waves and storms. They provide valuable ecosystem functions and are home to a large number of plants and animals. The degradation of vegetation caused by urban expansion is mainly expressed in two aspects: increasing built-up areas for human living and infrastructure probably reduces vegetation area; with economic development, the construction of ports for shipping extension and the expansion of aquaculture destroys coastal vegetation, which are crucial elements in stabilizing land surfaces against wind erosion and providing habitats for wildlife [14]. For example, mangrove forests in Southeast Asia experienced a significant decrease between 2000 and 2012 due to human activities and the expansion of aquaculture [15].

So far, several products obtained from remote-sensing techniques have been used to indicate vegetation conditions, such as vegetation indices, which can not only provide historical records of vegetation activities but also trace spatial development conditions and changes. The enhanced vegetation index (EVI) expresses a good dynamic range and sensitivity for monitoring and assessing spatial and temporal variations in vegetation conditions. EVIs are generally less likely to become saturated in high-biomass areas and also exhibit a smoother, more symmetrical seasonal profile with a narrower, well-defined peak greenness period [16].

Substantial research has been conducted to explore the impacts of urbanization on vegetation conditions at the local level [17–19]. Du et al. [20] found that urbanization caused a decrease in vegetation coverage in built-up areas for most of the central and eastern metropolises in China; the opposite was true in Western China because of the harsh natural environments. For 59 African cities that were averaged, the percentage of urban areas with a significant decreasing trend of annual vegetation coverage was 60%; cities near the Gulf of Guinea illustrated the most significant decrease in vegetation coverage [21]. Wetland vegetation declined to one-third between 1945 and 2007 [22], which was under constant threats from urbanization and other anthropogenic pressures in Greece. These results provide useful references for managers to recognize how policies and socioeconomic requirements influence ecosystems. However, what could be the effects of urban expansion on overall vegetation conditions in coastal cities?

Nowadays, more than half of the world's population live in urban areas, and by 2050, it is projected that this number will increase by more than two-thirds [23]. Of the world's population, about 40% live in coastal areas, a number which is growing, increasing pressures on coastal ecosystems. Among these pressures, habitat conversion, land-cover change, vegetation degradation and species invasion are of the greatest concern. The MSR has special economic and ecological characteristics, and covers a wide range of climates, ranging from subtropical to tropical, desert and Mediterranean. These push the investigation of vegetation from coastal city urbanization along the MSR.

In this study, we investigated the urbanization effects on vegetation in 35 coastal cities. First, built-up areas were obtained using a random forest (RF) algorithm for 35 coastal cities along the MSR between 2000 and 2015. Then, urban development intensity (UDI) was calculated using land-cover maps according to $1 \times 1 \text{ km}^2$ windows; UDIs were then divided into five zones for all the selected coastal cities. Third, the temporal developments of the EVI/EVI in urban zones against that in the rural area (ΔEVI) were analyzed. Finally, we calculated the spatial vegetation conditions from 2000 to 2015 across the MSR. The main objective of this study was to assess the effects of coastal urbanization on vegetation

dynamics under different UDI gradients. In particular, we would expect to: (1) unveil the EVI trends alongside rising urban development, (2) determine changes in vegetation along UDI gradients during 16 years across 35 coastal cities along the MSR and (3) quantify the relationship between vegetation activities and urbanization. Generally, this research highlights changes in vegetion conditions as urbanization increases, providing a reliable database for urban planning in the future.

2. Study Area

Geographically, the selected 35 port cities along the MSR cover 23 countries from Asia, Africa and Europe (Table 1, Figure 1). There were eight megacities [24] included in this study: Shenzhen (China), Manila (Philippines), Jakarta (Indonesia), Bangkok (Thailand), Kolkata (India), Mumbai (India), Karachi (Pakistan) and Istanbul (Turkey). The study area covers several climate zones that are different from eastern to western cities, and they are listed as subtropical, tropical, desert and Mediterranean climates. East Asia, Southeast and South Asia, with high vegetation coverage, belong to subtropical monsoon climates, tropical monsoon climates and tropical rainforest climates. West Asia and Africa are located in arid/semi-arid regions and are dominated by tropical desert climates. The selected coastal cities in Europe are mainly located around the Mediterranean Sea, with Mediterranean climates and large fluctuations in annual precipitation and temperature; the vegetation is mainly temperate mixed forests and temperate deciduous broad-leaved forests.
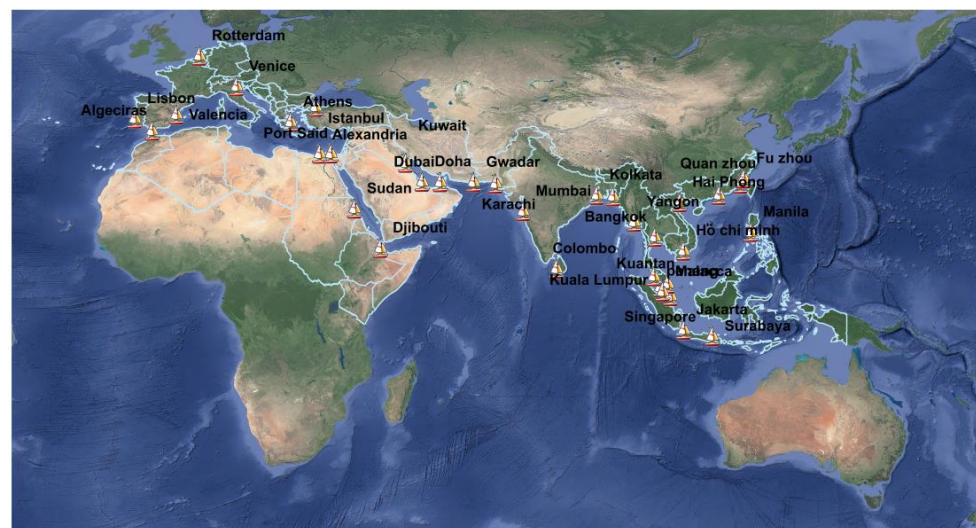

Figure 1. The selected 35 coastal cities along the study area. The background image is global satellite imagery (downloaded from ArcTiler Map).

The coastal area along the MSR has experienced economic development and has a large population as well as a huge port throughput. The primary products that are developed include agricultural product exports, industrial raw materials or product exports, tourism and shipping. The three economic corridors along the Indo-China Peninsula Economic Corridor, the Bangladesh–China–India–Burma Economic Corridor and the China–Pakistan Economic Corridor are the most dynamic regions for economic and trade relations between China and the countries along the route. Among them, Southeast Asia and South Asia have mild climates and developed agriculture industries; they are important global producers and exporters of food crops and tropical economic crops. Although the agricultural industries in West Asia and Africa are not well-developed, they are rich in natural resources, especially oil and minerals. They are also the world's major oil exporters and agricultural product import areas. Western Europe is considered the earliest region that underwent capitalist economic development. Its economies are among the world's largest, industrial development is mature, the production scale is huge, industry sectors are comprehensive, foreign trade is well-developed, natural and humanistic tourism resources

are abundant and tourism is well-developed. The development of industrial, agricultural and natural resources in various regions of the study area is expected to promote the development of the modern shipping industry and is the primary reason for the rapid development of coastal cities.

Table 1. The selected 35 coastal cities along the MSR.

Region		Country	ID	Coastal City
Asia	East Asia	China	1	Fuzhou
			2	Quanzhou
			3	Shenzhen
	West Asia	United Arab Emirates	4	Dubai
		Qatar	5	Doha
		Kuwait	6	Kuwait
	Southeast Asia	Philippines	7	Manila
		Indonesia	8	Surabaya
			9	Jakarta
		Vietnam	10	Hai Phong
			11	Ho Chi Minh
		Thailand	12	Bangkok
		Singapore	13	Singapore
		Malaysia	14	Kuantan
			15	Malacca
			16	Kuala Lumpur
			17	Penang
		Myanmar	18	Yangon
	South Asia	Bangladesh	19	Chittagong
		Sri Lanka	20	Colombo
		India	21	Kolkata
			22	Mumbai
		Pakistan	23	Karachi
			24	Gwadar
Africa		Djibouti	25	Djibouti
		Sudan	26	Port Sudan
		Egypt	27	Port Said
			28	Alexander
Europe		Turkey	29	Istanbul
		Greece	30	Athens
		Italy	31	Venice
		Spain	32	Valencia
			33	Algeciras
		Portugal	34	Lisbon
		The Netherlands	35	Rotterdam

3. Materials and Methods

3.1. Remotely Sensed Image Acquisition and Processing

We obtained land-cover maps of the selected 35 coastal cities for the years of 2000, 2010 and 2015 from Landsat TM/ETM+/OLI images (http://glovis.usgs.gov, accessed on 25 November 2021) with a spatial resolution of 30×30 m^2. The boundaries of these 35 coastal cities were defined according to the GADM (Global Administrative) dataset downloaded from the GADM website (www.gadm.org, accessed on 25 November 2021). Radiometric calibration, atmospheric correction, registration, mosaicking and subsetting were applied before land-use classification. An RF algorithm was used for the land-use classification. There were five land-use classes, i.e., built-up area, bare land, vegetation, water body and other land. Additionally, an accuracy assessment was done via validation plots obtained from Google Maps and quantified using the kappa coefficient and overall accuracy. With a spatial resolution of 1 km and a 16-day interval, MODIS EVI (MOD13A2) was used to monitor vegetation activities and dynamics from 2000 to 2015 in the 35 coastal cities. The average annual EVIs for each coastal city from 2000 to 2015 were calculated for further analysis, including temporal EVI trends and the relationship between the EVI and UDI:

$$\text{EVI} = \text{G} \times \frac{(\text{N} - \text{R})}{(\text{N} + \text{C1} \times \text{R} - \text{C2} \times \text{B} + \text{L})} \qquad (1)$$

where N/R/B are atmospherically corrected and partially atmosphere-corrected surface reflectances in near-infrared, red and blue bands, respectively; C1 and C2 are the coefficients of the aerosol resistance term; L is the canopy background adjustment that addressed nonlinear, differential N and R radiant transfer through a canopy. The coefficients adopted in the EVI are G (gain factor) = 2.5, C1 = 6, c2 = 7.5 and L = 1.

The UDI was defined as the proportion of built-up areas in each 1×1 km^2 grid based on 30×30 m^2 urban land-cover maps [25]. UDIs were calculated using a 1×1 km^2 window (in order to keep accordance with the size of the MODIS EVI pixels) for the years of 2000, 2010 and 2015. We stratified the urban area into five zones according to the UDIs [25]. From the lowest to the highest UDI in a city, the five zones were rural (UDI ≤ 0.05), exurban ($0.05 < \text{UDI} \leq 0.25$), suburb ($0.25 < \text{UDI} \leq 0.5$), urban ($0.5 < \text{UDI} \leq 0.75$) and urban core ($0.75 < \text{UDI} \leq 1$). We have assumed that the UDI maps in 2000, 2010 and 2015 could be used to symbolize the periods of 2000 to 2005, 2005 to 2010 and 2010 to 2015, respectively.

3.2. EVI Trends along Different UDI Gradients

Typically, the EVI declined with an increasing UDI, which meant that the EVI in urban cores had the lowest value among the zones. However, the EVI decaying modes varied with cities [26,27], and a nonlinear relationship between the EVI and UDI usually occurred due to seasonal variation, climate change and human interference. In view of this, we applied three possible forms in this study to express the relationship between the EVI and UDI (EVI–UDI) according to Zhou et al. [25], called Linear, Convex and Concave, to distinguish the performance of the EVI among different cities. Linear tells us that the EVI decreased linearly with a rising UDI. Convex means a slight downward curve, that is, it shows that the EVI decreased obviously alongside an increasing UDI. However, the EVI declined with a small slope first, which was then followed by a faster decrease with an increasing UDI. This trend always occurs in the coastal cities with a higher EVI intensity for vegetation pixels in the exurban or suburban than those in rural zones. The opposite is Concave, suggesting a sharp decrease in EVI first; the EVI trend then deceases slightly (Figure 2). A Concave pattern reflects strong vegetation activities in rural areas.
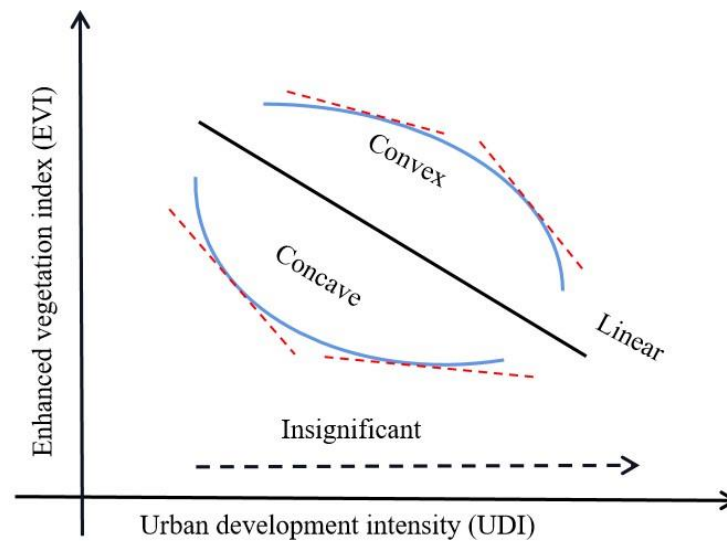
Figure 2. Forms of EVI–UDI models.

A quadratic regression analysis was calculated for each city to test the Convex or Concave trend:

$$y = ax^2 + bx + c, \text{ where a} \neq 0 \qquad (2)$$

where a indicates that the EVI was Convex (a < 0) or Concave (a > 0). The absolute value of a represents the convexity or concavity.

We calculated annual average EVIs with different UDI zones of 35 coastal cities in the period of 2000–2015. To avoid the potential effects of annual climate variations on the EVI [28], we hypothesized that the impact of urbanization on rural zones was minimal and that the background EVI could be represented by a rural EVI. Differences between an EVI with four urban zones (exurban, suburban, urban and urban core) and a rural EVI (called ΔEVI) were calculated, respectively, and temporal trends of ΔEVI over 2000 and 2015 were analyzed using linear regression.

4. Results and Discussion

4.1. Urban Change Mapping and Accuracy Assessment

Land-cover types common between all 35 coastal cities were classified into five classes (built-up, vegetation, water, bare land and others) using a random forest algorithm in the years 2000, 2010 and 2015. The accuracy assessment was performed for built-up areas based on Google Earth high-resolution images and a point-by-point verification approach. We generated 200 random verification points for each city and extracted corresponding points in land-cover maps; a confusion matrix was then used to evaluate the classification accuracy. For most coastal cities (60%, 21 out of 35), the kappa coefficients of urban built-up areas were greater than 0.90, and a few (10%) were lower than 0.70. The overall accuracy of the 35 coastal cities was 0.85, which met the accuracy requirement of land-use/cover change evaluation [29]. Coastal cities with high classification accuracy were mainly distributed in East Asia, Southeast Asia and South Asia, while coastal cities with low accuracy were mainly distributed in West Asia and Africa. This resulted from the fragmentation of built-up areas and the confused spectral features of unused land. Figure 3 shows the land-cover classifications of four representative coastal cities (Shenzhen, China; Singapore, Singapore; Dubai, United Arab Emirates; and Istanbul, Turkey) in the years of 2000, 2010 and 2015.

4.2. EVI Temporal Trend along UDI Gradients

As shown in Figure 4 and Table 2, the rural EVI and ΔEVI in four urban zones were analyzed using a linear regression model. The trends of the ΔEVI varied greatly among different coastal cities and urban zones between the years of 2000 and 2015. In most coastal cities, the ΔEVI in the four urban zones performed negatively, especially in urban and

urban core zones, with low absolute values (ΔEVI) in exurban and high absolute values in urban core zones. However, Surabaya (Indonesia), Doha (Qatar), Kuwait (Kuwait) and Port Sudan (Sudan) displayed positive ΔEVI in urban and urban core zones and had no obvious reduction even in urban core zones (Table 2), which indicated better vegetation conditions in those zones than in rural zones for those cities. For Surabaya (Indonesia), we found that the built-up area increased between 2000 and 2015, calculated from the land-cover maps, accompanied with significantly rising grassland in urban and urban core zones.
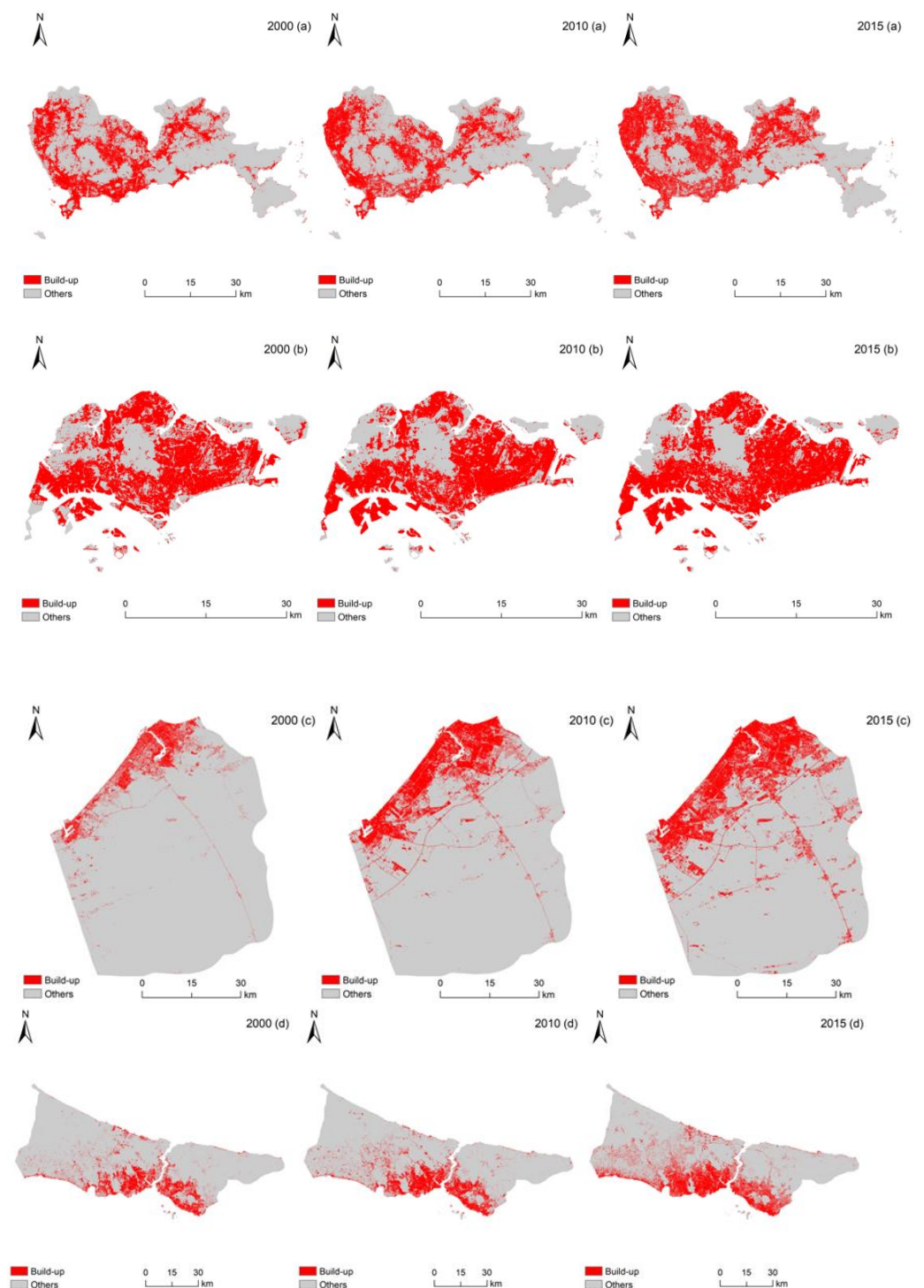

Figure 3. Built-up areas of four representative coastal cities along the MSR in 2000, 2010 and 2015. (**a**): Shenzhen, China; (**b**): Singapore, Singapore; (**c**): Dubai, United Arab Emirates; and (**d**): Istanbul, Turkey.

Table 2. Linear regression test of the temporal trends of rural EVI and the ΔEVI in four urban zones responding to the base rural condition for the 35 coastal cities from 2000 to 2015.

Region	ID	Coastal City	Rural		Exurban		Suburban		Urban		Urban Core	
			R	Slope	R	Slope	R	Slope	R	Slope	R	Slope
East Asia	1	Fuzhou	0.791 ***	0.0017	0.611 ***	0.0068	0.505 **	0.004	0.554 ***	0.007	0.441 **	0.004
	2	Quanzhou	0.711 ***	0.0036	0.568 ***	0.0044	0.006	−0.0002	0.199	−0.0013	0.884 ***	−0.007
	3	Shenzhen	0.669 ***	0.0046	0.268 *	0.0011	0.021	−0.0003	0.367 *	−0.002	0.577 ***	−0.003
Southeast Asia	4	Manila	0.491 ***	0.003	0.717 ***	−0.005	0.668 ***	−0.004	0.282 *	−0.001	0.533 ***	−0.003
	5	Surabaya	0.342 *	−0.003	0.638 ***	0.008	0.454 **	0.004	0.426 **	0.004	0.063	0.001
	6	Jakarta	0.687 ***	−0.021	0.705 ***	0.021	0.665 ***	0.021	0.679 ***	0.022	0.668 ***	0.020
	7	Hai Phong	0.140	0.0019	0.072	−0.0005	0.531 ***	0.006	0.455 **	0.008	0.290 *	−0.002
	8	Ho Chi Minh	0.613 ***	0.002	0.182	0.0001	0.393 **	−0.001	0.303 *	−0.001	0.213	−0.001
	9	Bangkok	0.018	0.0001	0.142	0.001	0.123	0.001	0.197	0.001	0.103	0.0001
	10	Singapore	0.003	0.0001	0.651 ***	0.004	0.162	0.001	0.149	0.001	0.318 *	0.002
	11	Kuantan	0.385	0.001	0.472 **	0.005	0.333 *	0.003	0.041	−0.001	0.086	−0.001
	12	Malacca	0.444 **	0.0016	0.377 *	0.001	0.502 **	0.0029	0.207	0.0014	0.006	−0.0002
	13	Kuala Lumpur	0.851 ***	0.0022	0.341 *	0.002	0.383 *	0.0026	0.050	0.0005	0.495 **	−0.001
	14	Penang	0.348 *	−0.001	0.055	0.0001	0.000	0.00002	0.560 ***	0.005	0.599 ***	0.003
	15	Yangon	0.564 ***	0.002	0.820 ***	0.002	0.546 ***	0.002	0.419 **	−0.001	0.609 ***	−0.002
South Asia	16	Chittagong	0.094	0.0005	0.736 ***	−0.0017	0.292 *	0.0024	0.334 *	0.003	0.496 **	−0.002
	17	Colombo	0.497 **	0.0022	0.552 ***	0.003	0.136	0.0013	0.114	0.002	0.023	0.0007
	18	Kolkata	0.241	−0.008	0.493	0.010	0.337	0.007	0.336	0.009	0.381 *	0.010
	19	Mumbai	0.200	0.002	0.295 *	−0.0001	0.450 **	0.001	0.395 **	0.002	0.261 *	−0.001
	20	Karachi	0.172	0.0015	0.014	−0.0001	0.034	0.0003	0.003	0.00009	0.266 *	−0.002
	21	Gwadar	0.502 **	0.0008	0.652 ***	0.003	0.476 **	−0.009	/	/	/	/
West Asia	22	Dubai	0.421 **	0.002	0.417 **	−0.0004	0.942 ***	0.0013	0.959 ***	0.002	0.917 ***	0.0014
	23	Doha	0.001	−0.00003	0.327 *	−0.001	0.583 ***	−0.002	0.081	0.0001	0.072	0.0001
	24	Kuwait	0.022	−0.0001	0.55 **	0.001	0.673 ***	−0.001	0.620 ***	0.002	0.174	−0.0005
Africa	25	Djibouti	0.253 *	−0.001	0.294 *	−0.0014	0.499 **	−0.002	0.711 ***	0.002	0.821 ***	0.002
	26	Sudan	0.028	−0.0001	0.706 ***	−0.001	0.007	0.00005	0.166	−0.0003	0.070	0.0003
	27	Port Said	0.906 ***	0.004	0.342 *	0.001	0.463 **	−0.003	0.806 ***	−0.004	0.849 ***	−0.004
	28	Alexander	0.079	0.0002	0.837	0.0017	0.766 ***	−0.001	0.124	−0.00024	0.130	0.0001
Europe	29	Istanbul	0.641 ***	0.003	0.352 *	0.0015	0.275 *	0.001	0.018	−0.00022	0.593 ***	−0.002
	30	Athens	0.678 ***	0.003	0.450 **	0.0009	0.408 **	0.001	0.177	0.0007	0.256 *	−0.001
	31	Venice	0.279 *	0.002	0.756 ***	0.001	0.112	0.0001	0.269 *	0.001	0.371 *	0.001
	32	Valencia	0.336 *	0.0035	0.035	0.0004	0.433 **	0.004	0.207	0.002	0.409 **	0.004
	33	Algeciras	0.001	−0.00003	0.229	0.0009	0.383*	0.0012	0.443**	0.0016	0.202 *	0.001
	34	Lisbon	0.342 *	0.003	0.058	0.0001	0.464**	−0.001	0.262*	−0.001	0.455 **	−0.003
	35	Rotterdam	0.434 **	0.004	0.002	0.0001	0.568***	−0.004	0.652***	−0.005	0.555 ***	−0.004

*** Significant at the 0.001 level. ** Significant at the 0.01 level. * Significant at the 0.05 level.
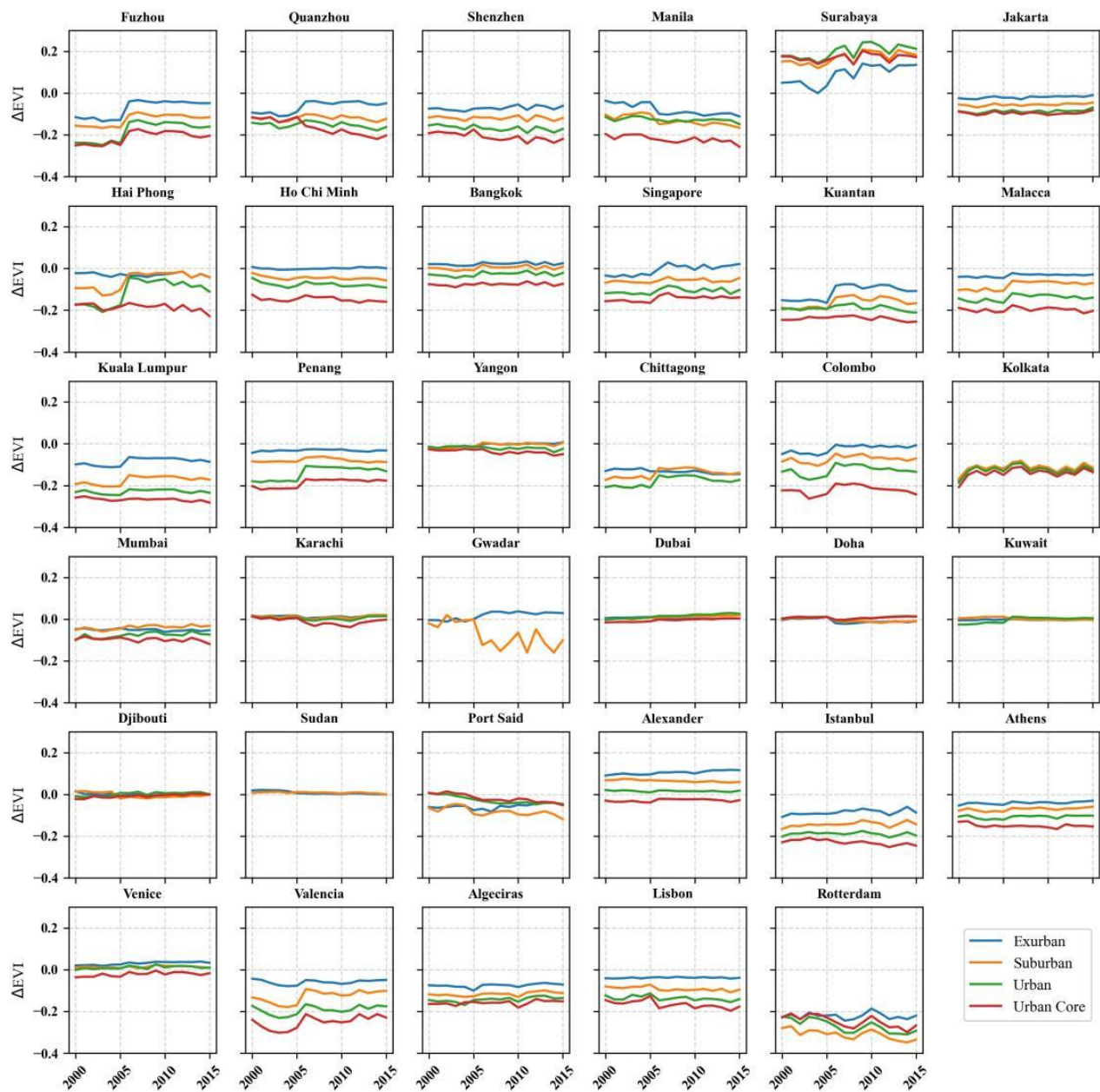
Figure 4. The ΔEVI of different urban zones from 2000 to 2015 for the 35 coastal cities.

Rural zones in Doha, Kuwait and Port Sudan were defined as desert or barren regions according to the UDI in this study; therefore, urban and urban core zones had higher EVI values than rural areas did (ΔEVI > 0). According to Van Vliet [30], these coastal cities experienced small expansions of their built-up areas. The rural EVI was stabler than that in urban zones [21], and the infill land development dominated in these cities due to their special desert geographical features [31]. In particular, Doha and Kuwait have had substantial population growth (natural growth and inward immigration) in recent decades, which was closely related to socioeconomic transformation since the exploration and exporting of fossil fuel in large volumes from around 1960 [32–34]. In regard to urban expansion, Doha has had a high rate of increase based on the land-cover maps and a large increase in recreational spaces (park, playgrounds) in urban zones, which exhibited sustainable urban development planning to improve living standards and the ecological environment [32]. Urbanization in Kuwait differed from that in Doha, having had rapid population growth but a relatively small increase in urban areas during recent decades. The city of Port Sudan underwent forced small north–south expansion in infrastructure

(e.g., transport, telecommunications and oil pipelines) because of the Red Sea to the east and mountains to the west [35].

The density of built-up areas in Gwadar increased because of the construction of residences and roads since the 2000s; additionally, with the development of the China–Pakistan Economic Corridor, port areas grew dramatically (0.06% per year) since 2014 [36]. It had a relatively low built-up density compared with that of other coastal cities in this study. Therefore, Gwadar did not have urban and urban core zones according to the UDI divisions, and the ΔEVI in exurban zones was positive. Coastal cities in Western Europe saw continued rural-to-urban migration due to their populations seeking better socioeconomic opportunities; the ΔEVI in urban core zones for the four European coastal cities displayed a negative and obvious declining trend.

A trend analysis of the EVI/ΔEVI in all zones from 2000 to 2015 was conducted (Table 2). Generally, the rural EVI for half of the coastal cities (18 of 35) increased significantly. The ΔEVI presented a decreasing trend only for a few cities in exurban (7 of 35), suburban (10 of 35) and urban (7 of 35) zones. However, half of the cities indicated a declined ΔEVI in urban core (14 of 35) zones with an average decreasing rate of 0.024/yr. Quanzhou city showed the maximal ΔEVI decreasing rate of 0.007/yr in its urban core. Four cities (Kuala Lumpur, Karachi, Istanbul and Athens) presented an obvious decrease in ΔEVI in urban core zones only, and two cities (Shenzhen and Yangon) showed a significant decrease in the ΔEVI in urban and urban core zones.

These may be attributed to two reasons: (1) relatively stable vegetation conditions in the rural zones of most of the cities; (2) most coastal cities exhibited an edge-expansion pattern in recent years which meant that built-up zone expansion mainly occurred in exurban and suburban zones. Salvati et al. [37] also found that vegetation condition is closely correlated with urban development mode through two Mediterranean regions (Athens and Rome). Notably, Bangkok had no apparent trend of rural EVI and ΔEVI in all urban zones. Manila exhibited a remarkable downward trend of the ΔEVI in all urban zones; in contrast, Fuzhou and Jakarta presented an obvious increase in the ΔEVI in all urban zones. Huang et al. [38] pointed out that the landscape patch index in western Fuzhou increased because of the increase in the urban green space, which may demonstrate the combined effects of urban sprawl and green space development. Jakarta experienced huge urbanization in recent years and was challenged by traffic congestions and floods [39]; additionally, Haughton and Hunter [40] implied that urbanization causes the countryside to lose its distinctive characteristics. This created a non-adaptive issue of the UDI zoning in this study, especially for agricultural cities similar to Jakarta.

4.3. Spatial Trends of Average EVI under Different Urban Gradients

According to the quadratic regression analysis (Figure 5), the averaged EVI over half of the coastal cities (19 of 35) declined significantly as the UDI increased ($p < 0.05$) from 2000 to 2015. The changed EVI rates in six cities (Port Said, Sudan, Kuwait, Doha, Jakarta and Surabaya) were positive, which meant good vegetation conditions in urban zones or a harsh desert environment (e.g., Kuwait, Sudan and Doha) in rural areas. Generally, the coastal cities with a high rate of decay of the EVI were mainly distributed in humid Asian areas. These results indicated that the decaying rate of the EVI correlated highly with climate conditions (temperature and precipitation) due to the responses of vegetation activities to climate change [41]. In some arid and semi-arid regions, Southern Africa and the Central East, for example, precipitation mainly occurred in rainy seasons, and vegetation conditions differed by season [42]; therefore, it is necessary to analyze the changed EVI rates seasonally in further research. The effects of urbanization on vegetation also varied with different vegetation types in different regions: for example, urbanization decreased cropland in Africa, and it will occupy 1.8–2.4% of cropland by 2030 [43]. The specific study of various vegetation types which are possibly influenced by urban expansion is helpful for policy decisions and urban planning.
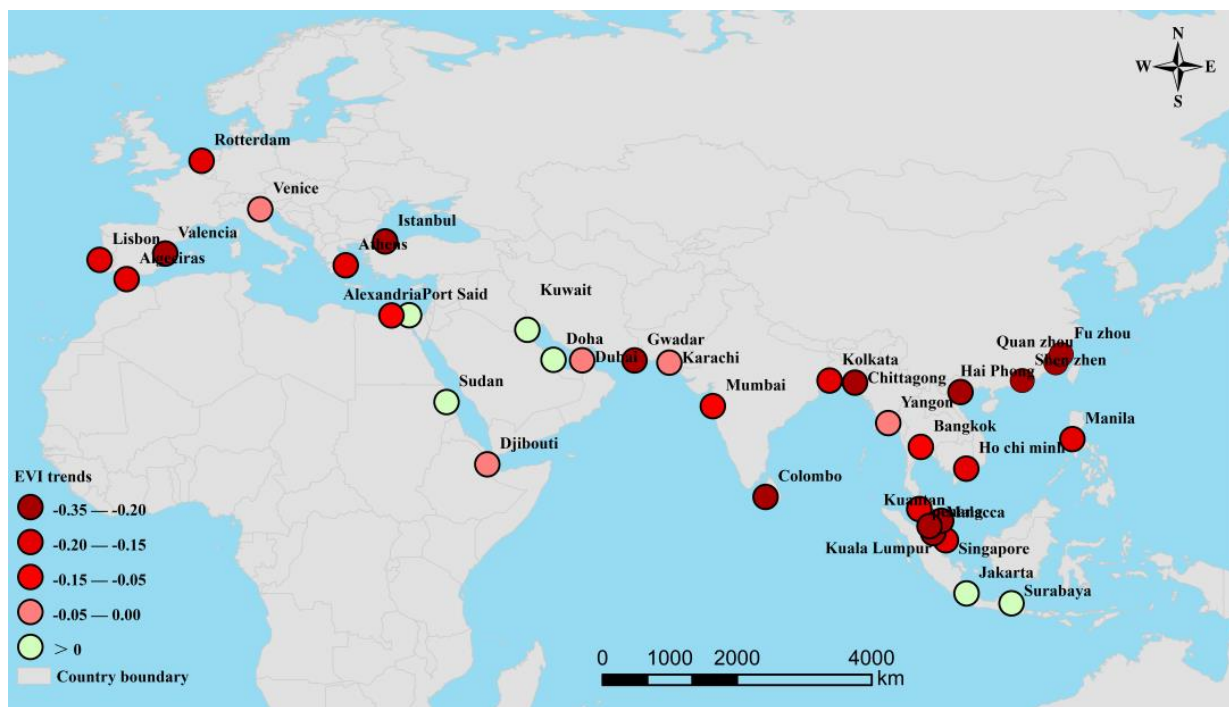
Figure 5. Spatial distribution of the EVI trends of the 35 coastal cities during the period of 2000–2015.

We classified the significant decreases in the EVI into three types: Linear, Concave and Convex (Figures 6 and 7). Linear-type cities (12 cities along the MSR) were assembled in Southeast and South Asia (10 of 12 cities); a Concave type occurred in seven cities: Fuzhou, Quanzhou, Shenzhen, Istanbul, Athens and Algeciras; and only one coastal city (Bangkok) showed a Convex trend. EVI–UDI trends in 15 cities were statistically insignificant, which were mainly located in the western region of the MSR. Previous knowledge from Imhoff et al. [44] and Sun et al. [45] implies that insignificant changes in the EVI appear in a few dry cities where the urbanization is not too intense and that vegetation conditions improve because of human irrigation and cultivation of suitable plant species.

Among the relationship between the EVI and UDI, linear models showed that the EVI linearly reduced alongside the increasing UDI in Asia. Urban development came at the direct price of losing agricultural land and foreshores, because many cities in Southeast Asia were dominated by paddy fields [46].

The Concave and Convex modes indicated that vegetation greenness was affected by many complex reasons involved in climate change and human activities over a long period of time; therefore, not all the modes were linear in coastal cities with various geographical regions. For instance, Bangkok showed a Convex pattern possibly because of intensive agriculture practices and land green space management in urban fringes [47], which might have had higher vegetation cover compared with that in the rural zone. Recently, Bangkok had experienced rising fragmentation and shape complexity of rural landscapes, and the urbanization mainly exhibited the conversion of agriculture into built-up zones in rural areas.
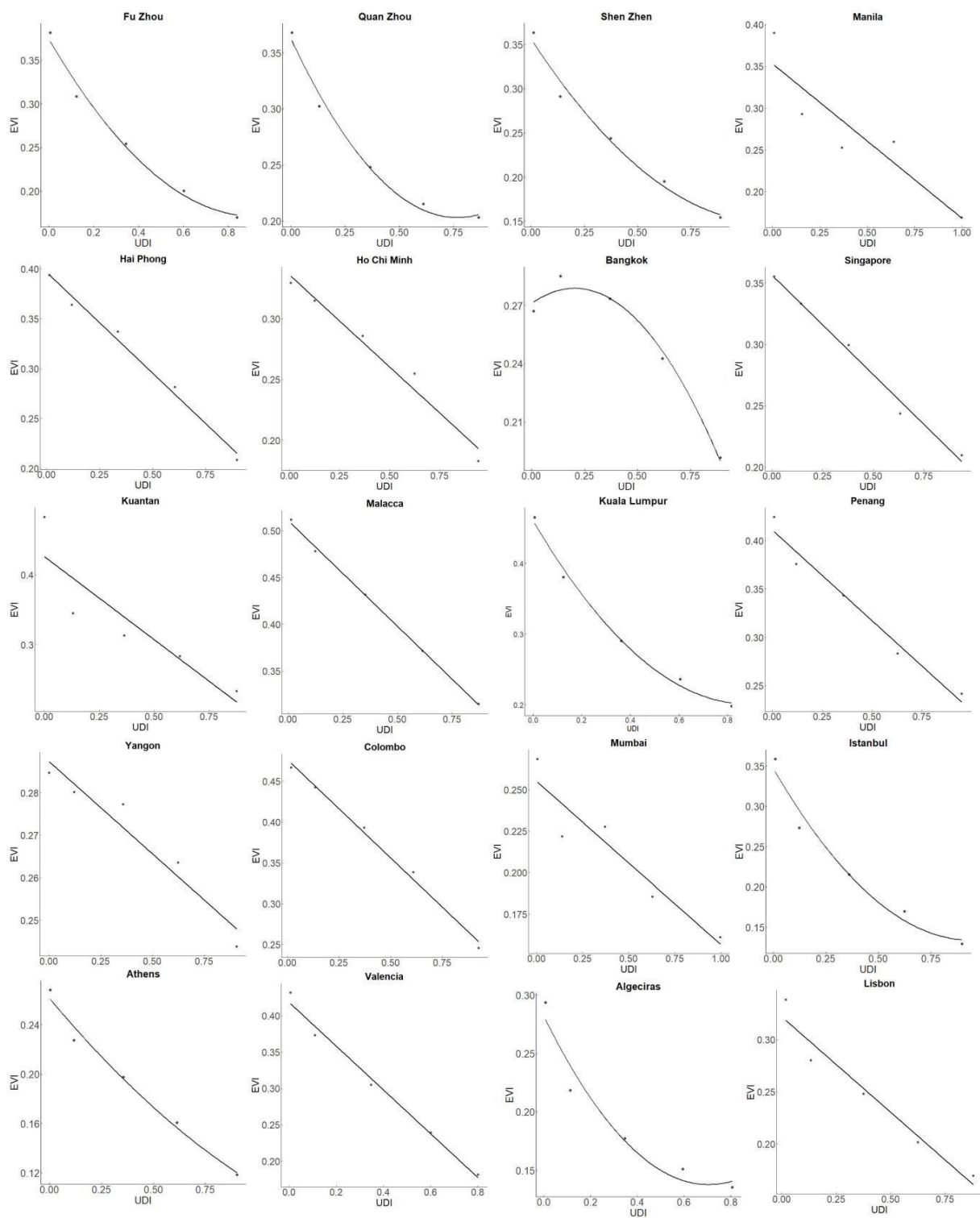
Figure 6. Curves of the EVI–UDI models of the 35 coastal cities during the period of 2000–2015.
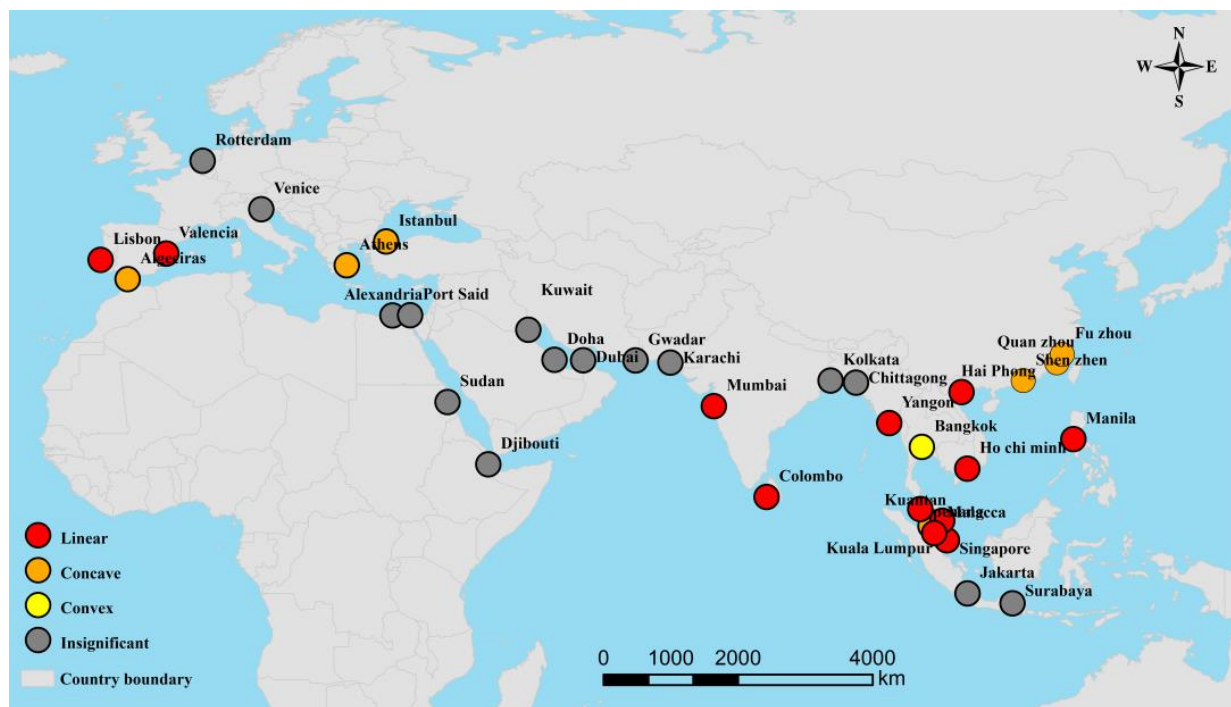
Figure 7. Spatial distribution of the EVI–UDI models of the 35 coastal cities during the period of 2000–2015.

5. Conclusions and Future Perspective

Coastal zones are unique areas with combinations of terrestrial, atmospheric and marine systems. Cities as important elements in coastal areas have experienced urban expansion in recent decades, and systematic analyses of coastal cities along the MSR are rare. From this perspective, we applied land-cover maps and MODIS time series EVI data to reveal the impacts of urbanization on vegetation conditions in 35 coastal cities along the MSR in this study. We analyzed the EVI/ΔEVI temporal trends in various zones from 2000 to 2015 and then developed EVI–UDI modes to clarify the relationship between the EVI and UDI for the coastal cities in order to explore regular EVI spatial trends along different zones. We found a significant reduction ($p < 0.05$) in the ΔEVI for almost half of the cities and an insignificant change in vegetation in the peri-urban areas or urban outskirts. The EVI decreased significantly alongside the UDI gradients in 12 coastal cities, with a linear pattern dominating in Asian cities; EVI trends in 15 cities were statistically insignificant. Overall, the results varied because of several factors, such as climate change and uncertainties induced by human activities. Therefore, urban planning policies and developmental stages influenced vegetation changes in cities; these findings could provide a scientific basis and decision-making reference for municipal urban planning, as well as scientific guidance for sustainable urban development.

Remaining uncertainties exist from this research. First, since the EVI–UDI mode differs across large areas under various climate conditions, the divisions of the UDI might be specified in the future for a particular region. Second, vegetation EVIs are seasonally various, especially in arid and semi-arid regions. The annual average EVI may influence actual EVI values. Third, we assumed the rural EVI as a stable background; however, the results from this study demonstrated that the rural EVI increased in most cities and that the ΔEVI values in the urban zones might be overestimated. More future work is necessary to quantify the climatic and environmental effects (e.g., extreme climate, land surface temperature) on vegetation conditions as well as understand the possible driving forces to urban vegetation. This is particularly the case for coastal cities as they are growing faster than inland cities because ports boost economic growth, generating substantial cargo transportation and job opportunities. Aside from the normal influences, vegetation

in coastal cities is vulnerable to ocean impacts, such as rises in sea level. Additionally, the consequences of decreased vegetation greenness, increased urban heat island and air pollution as well as reduced grain output need to be quantified in the future.

The rural–urban gradient is the most commonly applied methodology, considered to be a linear transect radiating out from the city core to the altered area. However, quantifying the effects of urbanization, especially the expansion of coastal cities, on vegetation systems in the rural–urban gradient is difficult because the gradient is a complicated integration of land uses [41]. How and to what extent the urbanization of coastal cities may affect vegetation would need to be included in future work.

References

1. Barragan, J.M.; de Andres, M. Analysis and trends of the world's coastal cities and agglomerations. *Ocean Coast Manag.* **2015**, *114*, 11–20. [CrossRef]
2. Wang, L.; Zhu, Y.; Ducruet, C.; Bunel, M.; Lau, Y.-Y. From hierarchy to networking: The evolution of the "twenty-first-century Maritime Silk Road" container shipping system. *Transp. Rev.* **2018**, *38*, 416–435. [CrossRef]
3. Zhao, C.; Wang, Y.; Gong, Y.; Brown, S.; Li, R. The evolution of the port network along the Maritime Silk Road: From a sustainable development perspective. *Mar. Policy* **2021**, *126*, 104426. [CrossRef]
4. Zeng, Q.; Wang, G.W.; Qu, C.; Li, K.X. Impact of the Carat Canal on the evolution of hub ports under China's Belt and Road initiative. *Transp. Res. Part. E Logist. Transp. Rev.* **2018**, *117*, 96–107. [CrossRef]
5. Euzen, A.; Gaill, F.; Lacroix, D.; Cury, P. *The Ocean Revealed*; CNRS éditions: Paris, France, 2008; pp. 208–209.
6. Ascensão, F.; Fahrig, L.; Clevenger, A.P.; Corlett, R.; Jaeger, J.A.G.; Laurance, W.F.; Pereira, H.M. Environmental challenges for the belt and road initiative. *Nat. Sustain.* **2018**, *1*, 206–209. [CrossRef]
7. Li, X.; Damen, M.C. Coastline change detection with satellite remote sensing for environmental management of the Pearl River Estuary, China. *J. Mar. Syst.* **2010**, *82*, S54–S61. [CrossRef]
8. Irfan, M.; Houdayer, B.; Shah, H.; Koj, A.; Thomas, H. GIS-based investigation of historic landfill sites in the coastal zones of Wales (UK). *Euro-Mediterr. J. Environ. Integr.* **2019**, *4*, 1–10. [CrossRef]
9. Rees, W.E. Ecological Footprint, Concept of. In *Encyclopedia of Biodiversity*, 2nd ed.; Levin, S.A., Ed.; Academic Press: Waltham, MA, USA, 2013; Volume 2, pp. 701–713.
10. Davies, Z.G.; Edmondson, J.L.; Heinemeyer, A.; Leake, J.R.; Gaston, K.J. Mapping an urban ecosystem service: Quantifying above-ground carbon storage at a city-wide scale. *J. Appl. Ecol.* **2011**, *48*, 1125–1134. [CrossRef]
11. Oldfield, E.E.; Warren, R.J.; Felson, A.; Bradford, M. FORUM: Challenges and future directions in urban afforestation. *J. Appl. Ecol.* **2013**, *50*, 1169–1177. [CrossRef]
12. Doick, K.J.; Peace, A.; Hutchings, T.R. The role of one large greenspace in mitigating London's nocturnal urban heat island. *Sci. Total Environ.* **2014**, *493*, 662–671. [CrossRef]
13. Li, X.; Zhou, X.; Asrar, G.R.; Imhoff, M.; Li, X. The surface urban heat island response to urban expansion: A panel analysis for the conterminous United States. *Sci. Total Environ.* **2017**, *605–606*, 426–435. [CrossRef]
14. Asensi, A.; Garretas, B.D. Coastal vegetation. In *The Vegetation of the Iberian Peninsula*; Plant and Vegetation Volume 13; Loidi, J., Ed.; Springer: Utrecht, The Netherlands, 2017; pp. 397–432.
15. Richards, D.R.; Friess, D.A. Rates and drivers of mangrove deforestation in Southeast Asia, 2000–2012. *Proc. Natl. Acad. Sci. USA* **2016**, *113*, 344–349. [CrossRef]

16. Huete, A.; Didan, K.; Miura, T.; Rodriguez, E.P.; Gao, X.; Ferreira, L.G. Overview of the radiometric and biophysical performance of the MODIS vegetation indices. *Remote Sens. Environ.* **2002**, *83*, 195–213. [CrossRef]
17. Chen, B.; Nie, Z.; Chen, Z.; Xu, B. Quantitative estimation of 21st-century urban greenspace changes in Chinese populous cities. *Sci. Total Environ.* **2017**, *609*, 956–965. [CrossRef] [PubMed]
18. Nowak, D.J.; Greenfield, E.J. Tree and impervious cover change in U.S. cities. *Urban For. Urban Green.* **2012**, *11*, 21–30. [CrossRef]
19. Zhao, J.; Chen, S.; Jiang, B.; Ren, Y.; Wang, H.; Vause, J.; Yu, H. Temporal trend of green space coverage in China and its relationship with urbanization over the last two decades. *Sci. Total Environ.* **2012**, *442*, 455–465. [CrossRef] [PubMed]
20. Du, J.; Fu, Q.; Fang, S.; Wu, J.; He, P.; Quan, Z. Effects of rapid urbanization on vegetation cover in the metropolises of China over the last four decades. *Ecol. Indic.* **2019**, *107*, 105458. [CrossRef]
21. Yao, R.; Cao, J.; Wang, L.; Zhang, W.; Wu, X. Urbanization effects on vegetation cover in major African cities during 2001–2017. *Int. J. Appl. Earth Obs.* **2019**, *75*, 44–53. [CrossRef]
22. Krina, A.; Xystrakis, F.; Karantininis, K.; Koutsias, N. Monitoring and projecting land use/land cover changes of eleven large deltaic areas in Greece from 1945 onwards. *Remote Sens.* **2020**, *12*, 1241. [CrossRef]
23. Ritchie, H.; Roser, M.; Urbanization. Published Online at OurWorldInData.org. Available online: https://ourworldindata.org/urbanization (accessed on 10 November 2021).
24. United Nations, Department of Economic and Social Affairs, Population Division. *World Urbanization Prospects: The 2014 Revision, Highlights*; United Nations: New York, NY, USA, 2014.
25. Zhou, D.; Zhao, S.; Liu, S.; Zhang, L. Spatiotemporal trends of terrestrial vegetation activity along the urban development intensity gradient in China's 32 major cities. *Sci. Total Environ.* **2014**, *488–489*, 136–145. [CrossRef]
26. Yuan, F.; Bauer, M.E. Comparison of impervious surface area and normalized difference vegetation index as indicators of surface urban heat island effects in Landsat imagery. *Remote Sens. Environ.* **2007**, *106*, 375–386. [CrossRef]
27. Luck, G.W.; Smallbone, L.T.; O'Brien, R. Socio-economics and vegetation change in urban ecosystems: Patterns in space and time. *Ecosystems* **2009**, *12*, 604–620. [CrossRef]
28. Dallimer, M.; Tang, Z.; Bibby, P.R.; Brindley, P.; Gaston, K.J.; Davies, Z.G. Temporal changes in greenspace in a highly urbanized region. *Biol. Lett.* **2011**, *7*, 763–766. [CrossRef]
29. Janssen, L.L.F.; Vanderwel, F.J.M. Accuracy assessment of satellite derived land-cover data: A review. *Photogramm. Eng. Remote Sens.* **1994**, *60*, 419–426.
30. Van Vliet, J. Direct and indirect loss of natural area from urban expansion. *Nat. Sustain.* **2019**, *2*, 755–763. [CrossRef]
31. Shandas, V.; Makido, Y.; Ferwati, S. Rapid urban growth and land use patterns in Doha, Qatar: Opportunities for sustainability? *Eur. J. Sustain. Dev. Res.* **2017**, *1*, 11. [CrossRef]
32. Hashem, N.; Balakrishnan, P. Change analysis of land use/land cover and modelling urban growth in Greater Doha, Qatar. *Ann. GIS* **2015**, *21*, 233–247. [CrossRef]
33. Algharib, S.M. Spatial Patterns of Urban Expansion in Kuwait City between 1989 and 2001. Master's Thesis, Kent State University, Kent, OH, USA, 2008.
34. Alghais, N.; Pullar, D. Modelling future impacts of urban development in Kuwait with the use of ABM and GIS. *Trans. GIS* **2018**, *22*, 20–42. [CrossRef]
35. Ati, H.; Pavanello, S.; Jaspars, S.; Hashim, A. City Limits: Urbanisation and Vulnerability in Sudan, Port Sudan Case Study. 2011. Available online: http://dspace.cigilibrary.org/jspui/handle/123456789/31337. (accessed on 19 June 2012).
36. Zuo, J.; Bian, J.; Li, A.; Lei, G.; Wang, Z. Estimating Impervious Surfaces of Gwadar City Based on the Chinese Multi-Sources Remote Sensing Images. In Proceedings of the IGARSS 2018-2018 IEEE International Geoscience and Remote Sensing Symposium, Valencia, Spain, 22–27 July 2018; pp. 2631–2634. [CrossRef]
37. Salvati, L.; Zitti, M. Monitoring vegetation and land use quality along the rural–urban gradient in a Mediterranean region. *Appl. Geogr.* **2012**, *32*, 896–903. [CrossRef]
38. Huang, B.-X.; Chiou, S.-C.; Li, W.-Y. Landscape pattern and ecological network structure in urban green space planning: A case study of Fuzhou city. *Land* **2021**, *10*, 769. [CrossRef]
39. Maheng, D.; Pathirana, A.; Zevenbergen, C. A preliminary study on the impact of landscape pattern changes due to urbanization: Case study of Jakarta, Indonesia. *Land* **2021**, *10*, 218. [CrossRef]
40. Haughton, G.; Hunter, C. Urban Growth and the Urban Environment. In *Sustainable Cities*, 1st ed.; Routledge: London, UK, 2003.
41. Nemani, R.R.; Keeling, C.D.; Hashimoto, H.; Jolly, W.M.; Piper, S.C.; Tucker, C.J.; Myneni, R.B.; Running, S.W. Climate-driven increases in global terrestrial net primary production from 1982 to 1999. *Science* **2003**, *300*, 1560–1563. [CrossRef]
42. Rishmawi, K.; Prince, S.D.; Xue, Y. Vegetation responses to climate variability in the northern arid to sub-humid zones of Sub-Saharan Africa. *Remote Sens.* **2016**, *8*, 910. [CrossRef]
43. Bren D'Amour, C.; Reitsma, F.; Baiocchi, G.; Barthel, S.; Güneralp, B.; Erb, K.-H.; Haberl, H.; Creutzig, F.; Seto, K.C. Future urban land expansion and implications for global croplands. *Proc. Natl. Acad. Sci. USA* **2017**, *114*, 8939–8944. [CrossRef] [PubMed]
44. Sun, J.; Wang, X.; Chen, A.; Ma, Y.; Cui, M.; Piao, S. NDVI indicated characteristics of vegetation cover change in China's metropolises over the last three decades. *Environ. Monit. Assess.* **2011**, *179*, 1–14. [CrossRef]
45. Stutzer, D.; Lawrence, W.; Tucker, C.; Imhoff, M. The use of multisource satellite and geospatial data to study the effect of urbanization on primary productivity in the United States. *IEEE Trans. Geosci. Remote Sens.* **2000**, *38*, 2549–2556. [CrossRef]

46. Urbanization and Sustainability Asia. In *Urbanization and Sustainability in Asia: Case Studies of Good Practice*; Roberts, B.; Trevor, K. (Eds.) Asian Development Bank and Cities Alliance: Manila, Philippines, 2006; pp. 16–24.

47. NAGASAWA, R.; Patanakano, B. Urbanization and its Influences on the Suburban landscape changes in Bangkok Metropolitan region, Thailand. *J. Jpn. Agric. Syst. Soc.* **2013**, *29*, 29–39. [CrossRef]